Coupled Dielectric-Split Ring Microwave Resonator for Liquid Measurements in Microfluidic Channels at Nanoliter Volumes

C. Watts[1], S. M. Hanham[1], M. M. Ahmad[2], M. Adabi[1] and N. Klein[1]
[1] Department of Materials, [2] Department of Electrical and Electronic Engineering
Centre for Terahertz Science and Engineering
Imperial College London
London, UK
CW2313@ic.ac.uk

***Abstract*— A microwave dielectric resonator based sensor system has been investigated with respect to its sensitivity for the assessment of aqueous liquids. The system exploits the field enhancement of a split ring structure while retaining high and tunable quality factors due to weak and adjustable coupling between a planar split-ring and a dielectric resonator. The proposed sensor with integrated microfluidic channel allows investigation of volumes of liquids less than 1 nL and is capable of detecting small changes in relative permittivity, as demonstrated by measurements of water-ethanol solutions.**

Keywords*— Dielectric resonator, liquid dielectric sensor, microfluidic sensor, split-ring resonator

I. Introduction

Due to the strong interaction of water with electric fields at microwave frequencies, sensors operating in this regime have shown high sensitivity for the measurement of the complex dielectric permittivity (ε*) of small volumes of aqueous solutions [1-9]. This is promising for biosensing applications where most liquids to be investigated consist predominantly of water.

Coaxial probe approaches have shown to be sensitive to low concentrations of biomolecules over a broad frequency range, and concentration-independent differentiation between different dissolved protein species was demonstrated based on small variations in the real and imaginary components of ε* around the Debye relaxation frequency of water [1]. Microwave dielectric resonators (DRs) operating in whispering gallery modes at 10-40 GHz have been used to distinguish low concentrations of organic liquids and solutions of proteins, glucose (<0.1% w/w) and sodium chloride (70 ppt) using sub-nanoliter volumes of analyte [2], [3].

Other approaches using on-chip electrodes and microfluidic channels to concentrate electric fields around the liquid under test have achieved high sensitivity to ethanol solutions on volumes less than 0.5 nL [4] as well as showing promise for cell sensing [5]. Resonant split ring structures have also been used to demonstrate significant sensitivity for aqueous solutions of organic liquids and biomolecules [6]–[8].

This paper introduces a system which utilizes the electric field confining properties of a split ring and microfluidic channel system but avoids the implementation of microwave connectors on the microfluidic chip. This allows the microfluidic chips to be inexpensive and potentially disposable. The wireless method of excitation used in our system also helps to maintain relatively high and measurable Q-factors despite measurement of liquids with high loss tangents (>0.5).

II. Design of Coupled Dielectric-Split Ring Resonator

As shown in Fig 1, the proposed system consists of a microfluidic channel passing through the gaps of a metallic split ring (SR) deposited on a glass slide which sits on a circular aperture in a copper cavity housing a cylindrical dielectric resonator. The $TE_{01\delta}$ mode in the DR is excited via coaxial coupling loops. The coupling loops are adjusted for symmetric coupling and about -20 dB insertion loss for the case of the dielectric loaded cavity without the split ring in order to determine the resonant parameters from simple $|S_{21}|$ measurements. Figure 2b shows how the small magnetic field of the $TE_{01\delta}$ mode, which leaks through the aperture, induces an alternating current in the SR (Fig 2a). The displacement current across the capacitive gaps between the two half rings corresponds to a strong electric field confined in a small volume (Fig 3a). By controlling the size of the ring and the gap, the electric field can be confined to an arbitrarily small volume.

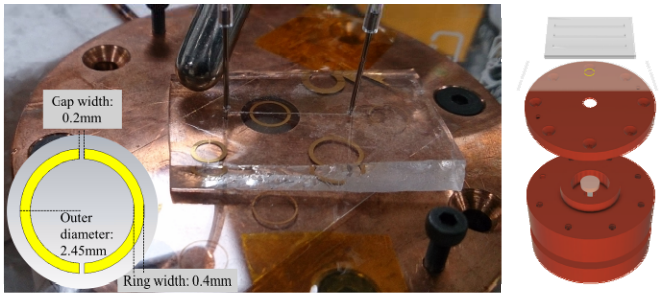

Fig. 1. Photograph of sensor set up (left), schematic showing the geometry of the split ring investigated (inset) and expanded schematic (right) showing, from bottom to top, copper housing, dielectric puck resonator mounted on a quartz column, lid with aperture, glass coverslip with metal split ring and the PDMS microfluidic channel.

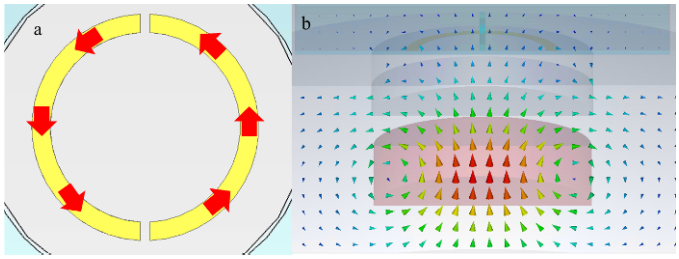

Fig. 2. a) Visualisation of the currents flowing in the split ring and b) CST Microwave Studio simulation showing the shape of the magnetic field of the dielectric puck which can be seen protruding out of the aperture and wrapping round the split ring.

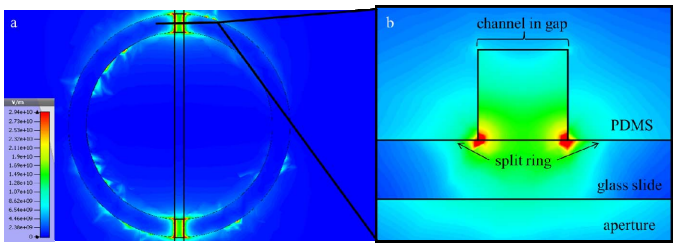

Fig. 3, Simulations (CST Microwave Studio): a) colour plot of the electric field strength showing enhancement of the electric field in the gaps of the ring and b) vertical cross section of the channel passing through the split ring gap (location of cross-section indicated on a) showing the distribution of electric field in the liquid.

The SRs are fabricated from gold deposited onto 130 µm thick borosilicate glass (BSG) coverslips. A schematic of the SR geometry is shown in Fig 1. Microfluidic channels are made in PDMS (polydimethylsiloxane) by pouring PDMS mixed with a crosslinking agent over a negative of the desired shape and leaving to cure overnight. Once removed from the mold the PDMS is flexible enough to make a semi-permanent seal with the glass coverslip. Connectors are punched through the PDMS mold and tubing is attached allowing the use of a pressure pump to control the flow of liquid samples through the channel. The channel is aligned with the SR gaps using an optical microscope and left to create a seal. The SR and channel arrangement is then placed on top of the copper cavity so that the SR is approximately in the centre of the aperture.

Placing or flowing liquid samples through the gaps changes the permittivity of the space between the gaps which dramatically changes the capacitance and the resistive load of the gaps, which translates into a directly measurable variation of the resonant frequency and quality factor of the coupled DR-SR assembly. Table 1 shows how different conditions affect the measured resonance frequency and quality factor.

III. Results and Discussion

Using a HP 8722 VNA measurements of the resonance frequency (fc) and quality factor (Q) were carried out on solutions of ethanol in deionized water of 4, 10 and 15% by volume by using an algorithm which fits a Q-factor circle in the polar S_{21} plane as described in [10]. Deionized water was measured before each sample as a reference. The change in resonant frequency f and inverse quality factor Q was calculated as:

TABLE I.

The relationship between different conditions and the resonance parameters of the coupled resonator system. The highest quality factor resonance is achieved when the dielectric resonator is operated on its own, without the split ring. Addition of the PDMS microfluidic chip does not significantly affect the resonance. The addition of the split ring causes a significant change in quality factor, as does the addition of water into the channel

Condition	Resonant Frequency (GHz)	Unloaded Quality Factor
Dielectric Puck	9.68237117	6412
Dielectric Puck + PDMS	9.68207061	6041
Dielectric Puck + Metal Ring + empty PDMS channel	9.648705027	1002
Dielectric Puck + Metal Ring + water in PDMS channel	9.708080567	104.3

$$\Delta f = f_{sample} - f_{water} \tag{1}$$

$$\Delta\left(\frac{1}{Q}\right) = \frac{1}{Q_{sample}} - \frac{1}{Q_{water}} \tag{2}$$

Subscripts denote measurements of either ethanol solution samples or water, the results are plotted as a function of the ethanol concentration in Fig 4.

The perturbation of the resonance due to the liquid samples can be expressed in units of the full width half maximum (FWHM) of the resonance. This normalized data helps to visualize how significant a shift is with respect to the width of the resonance and therefore presents a figure-of-merit for the sensitivity. For the normalized frequency shift Eq. 1 becomes

$$\frac{\Delta f}{FWHM_{water}} = \frac{\Delta f}{\frac{1}{Q_{water}} \times f_{water}} = \frac{\Delta f}{f_{water}} \times Q_{water} \tag{3}$$

and for the inverse Q-factor shift Eq. 2 can be expressed as:

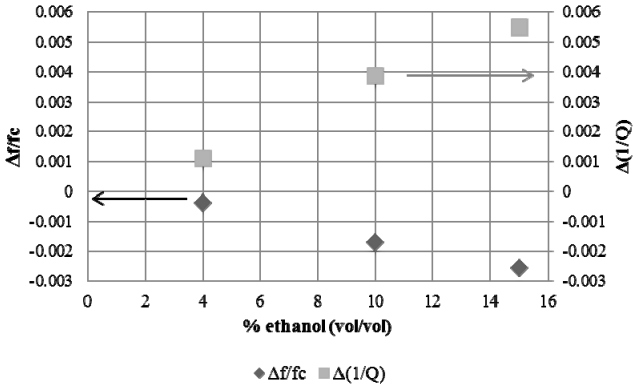

Fig. 4. Plot of the measured frequency shift (as a fraction of resonance with water in the channel) and reciprocal quality factor shift as a function of the concentration of ethanol in deionised water (volume %).

$$\frac{FWHM_{sample} - FWHM_{water}}{FWHM_{water}} = \frac{\frac{f_{sample}}{Q_{sample}} - \frac{f_{water}}{Q_{water}}}{\frac{f_{water}}{Q_{water}}} = \frac{Q_{water}}{f_{water}}\left[\frac{f_{sample}}{Q_{sample}} - \frac{f_{water}}{Q_{water}}\right] \quad (4)$$

The measured data is plotted as a function of ethanol concentration in Fig 5.

Literature data for the complex permittivity of the ethanol solutions [11] were used to calculate the loss tangent, as shown in Table 2, which can then be related to the measured normalized inverse quality factor shift, as shown in Fig 6. Further investigations of different aqueous solutions with different concentrations are currently in progress.

IV. Conclusions

The proposed system shows a high sensitivity to small changes in permittivity close to the permittivity of water which demonstrates it has potential as a sensor in biological systems. For example, a 4% solution of ethanol results in a normalized inverse quality factor shift of more than 10% and a normalized frequency shift of almost 5% away from that of water. This is a change in permittivity of less than 4% and is easily measureable.

As can be seen in Fig. 3 the volume of liquid exposed to the high electric field strength is quite small and corresponds roughly to the volume enclosed by the split ring. This gives a calculated interaction volume of less than 200 pL, showing that the system has clear potential for sensing of very small volumes of liquids, possibly down to single cell measurements.

The frequency shift observed from the resonator shows the opposite trend to what would be predicted from perturbation theory. This may be due to the variation of the coupling strength between the DR and the SRR owing to a change of the loading of the capacitive gaps caused by the liquid under test. This effect, as well as the high losses of the liquids tested means that the real and imaginary parts of the permittivity cannot be directly related to the changes in resonant frequency and quality factor, respectively. Currently an equivalent circuit model is being developed which takes into account a coupled resonator circuit and a transmission line model for the SRR to help explain this behavior. The circuit model could also elucidate the dependence of frequency and quality factor on real and imaginary permittivity, allowing the determination of the complex permittivity of liquids from measured values.

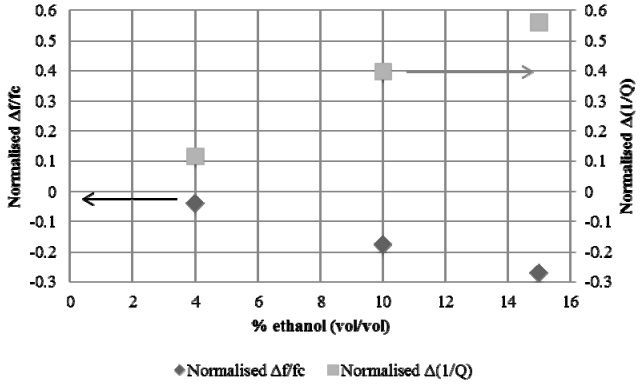

Fig. 5. Plot of frequency and quality factor shift in terms of the resonance half width against concentration of ethanol in deionised water (volume %).

TABLE II.

THE RELATIONSHIP BETWEEN ETHANOL SOLUTIONS AND PERMITTIVITY AND LOSS TANGENT. PERMITTIVITY DATA REPRODUCED FROM [11].

Sample	Real Permittivity (ε') at 10GHz	Imaginary Permittivity (ε'') at 10GHz	Loss tangent (tanδ = ε''/ε')
0% ethanol	60.6	32.4	0.53
4% ethanol	55.9	33.6	0.60
10% ethanol	48.8	33.9	0.69
15% ethanol	40	33.8	0.84

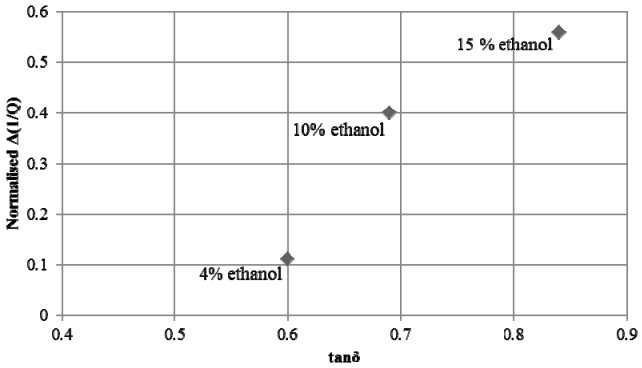

Fig. 6. Plot of normalized quality factor shift in terms of the resonance half width against loss tangent values for the different ethanol in deionised water solutions (volume %).

Acknowledgment

This work has been funded by the United Kingdom's Engineering and Physical Sciences Research Council (EPSRC) under the project code EP/M001121/1. Data supporting this publication can be obtained upon request from terahertz@imperial.ac.uk.

References

[1] T. H. Basey-Fisher, S. M. Hanham, H. Andresen, S. a. Maier, M. M. Stevens, N. M. Alford, and N. Klein, "Microwave Debye relaxation analysis of dissolved proteins: Towards free-solution biosensing," Appl. Phys. Lett., vol. 99, no. 23, p. 233703, 2011.

[2] E. N. Shaforost, N. Klein, S. a. Vitusevich, a. Offenhäusser, and a. a. Barannik, "Nanoliter liquid characterization by open whispering-gallery mode dielectric resonators at millimeter wave frequencies," J. Appl. Phys., vol. 104, no. 7, p. 074111, 2008.

[3] E. N. Shaforost, N. Klein, S. a. Vitusevich, a. a. Barannik, and N. T. Cherpak, "High sensitivity microwave characterization of organic molecule solutions of nanoliter volume," Appl. Phys. Lett., vol. 94, no. 11, p. 112901, 2009.

[4] T. Chretiennot, D. Dubuc, and K. Grenier, "A microwave and microfluidic planar resonator for efficient and accurate complex permittivity characterization of aqueous solutions," IEEE Trans. Microw. Theory Tech., vol. 61, no. 2, pp. 972–978, 2013.

[5] K. Grenier, D. Dubuc, P.-E. Poleni, M. Kumemura, H. Toshiyoshi, T. Fujii, and H. Fujita, "Integrated Broadband Microwave and Microfluidic

Sensor Dedicated to Bioengineering," IEEE Trans. Microw. Theory Tech., vol. 57, no. 12, pp. 3246–3253, Dec. 2009.

[6] W. Withayachumnankul, K. Jaruwongrungsee, A. Tuantranont, C. Fumeaux, and D. Abbott, "Metamaterial-based microfluidic sensor for dielectric characterization," Sensors Actuators, A Phys., vol. 189, pp. 233–237, 2013.

[7] A. a. Abduljabar, D. J. Rowe, A. Porch, and D. a. Barrow, "Novel microwave microfluidic sensor using a microstrip split-ring resonator," IEEE Trans. Microw. Theory Tech., vol. 62, no. 3, pp. 679–688, 2014.

[8] H. Torun, F. Cagri Top, G. Dundar, and a. D. Yalcinkaya, "An antenna-coupled split-ring resonator for biosensing," J. Appl. Phys., vol. 116, p. 124701, 2014.

[9] S. M. Hanham, C. Watts, W. J. Otter, S. Lucyszyn, and N. Klein, "Dielectric measurements of nanoliter liquids with a photonic crystal resonator at terahertz frequencies," Appl. Phys. Lett., vol. 107, no. 3, p. 032903, 2015.

[10] A. P. Gregory, "Q-factor measurement using a vector network analyser", NPL Report No. MAT 58, 2013.

[11] R. Olmi, V. V Meriakri, A. Ignesti, S. Priori, and C. Riminesi, "Monitoring alcoholic fermentation by microwave dielectric spectroscopy.," J. Microw. Power Electromagn. Energy, vol. 41, no. 3, pp. 37–49, 2007.